An Optimal Frequency Control Method Through a Dynamic Load Frequency Control (LFC) Model Incorporating Wind Farm

Vahid Gholamrezaie, Mehdi Ghazavi Dozein, Hassan Monsef, *Member, IEEE*, and Bin Wu, *Fellow, IEEE*

***Abstract*—In a high penetrated wind farm power system, wind farms can collaborate to control the power system frequency as like as conventional units. This paper presents a novel model to control the frequency of the wind farm connected to conventional units. Throughout the proposed frequency control, the integral controller, washout filter, and the PID controller could determine the active power variation value in different situations. In fact, a PID controller makes the wind farm aware of power variations. To improve the efficiency of the model, the defined frequency control parameters (i.e., PID coefficients) are optimized based on a multiobjective function using particle swarm optimization algorithm. This study has a unique perspective based on the wind farm collaboration through inertia control, primary frequency control, and supplementary frequency control of the system. A swift power reserve in a stable condition is needed in which wind farm can ameliorate the system frequency response. It is worth saying that the wind farm consists of variable speed turbines, such as a doubly fed induction generator, or a permanent magnet synchronous generator. To assess the performance of the proposed model, it is applied to a typical two-area system and the results are compared.**

***Index Terms*—Additional damping ($D_{\rm A}$), additional inertia ($M_{\rm A}$), doubly fed induction generator (DFIG), frequency control, load frequency Control (LFC), permanent magnet synchronous generators (PMSG).**

NOTATION

The notation used throughout this paper is reproduced below for quick reference.

ρ	Air density in kg/m^3.
A	The sweep area of wind turbine in m^2.
V_ω	Wind speed in m/s.
X	Coefficient to define reserve power in wind farm.
$P_{\rm opt}$	Optimum available wind power.
$P_{\rm res}^{-}$	Negative reserve power in wind farm.
$P_{\rm res}^{+}$	Positive reserve power in wind farm.
P_m	Mechanical input power of wind farm.
P_e	Electrical output power of wind farm.
ω_m	Mechanical rotational speed.
$\omega_{\rm ref}^{*}$	Mechanical reference rotational speed.
k_P	Speed regulator proportional constant.
k_i	Speed regulator integral constant.
J	Moment of inertia of the rotating mass.
ΔP_G	Active power variation of conventional generator.
$\Delta P_{\rm wind}$	Active power variation of wind farm.
ΔP_L	Active power variation of load.
Δf	Frequency variation.
$\Delta P_{\rm FC}$	Power response for frequency control.
M	Inertia constant.
D	Damping constant.
M_A	Additional inertia constant.
D_A	Additional damping constant.
K_P	Spinning reserve constant.
T_G	Governor time constant.
T_T	Turbine time constant.
R	Droop constant.
K	Supplementary control integral constant.

Manuscript received August 1, 2015; revised January 24, 2016 and March 27, 2016; accepted April 3, 2016. This work was supported by the Research Center of Power System Operation and Planning Studies, School of ECE, College of Engineering, University of Tehran, Tehran, Iran.

V. Gholamrezaie, M. Ghazavi Dozein, H. Monsef are with the School of ECE, College of Engineering, University of Tehran, Tehran 14395-515, Iran (e-mail: v.gholamrezaie@ut.ac.ir; m_ghazavi@ut.ac.ir; hmonsef@ut.ac.ir).

B. Wu is with the Department of Electrical Engineering, Ryerson University, Toronto, ON M5B 2K3, Canada (e-mail: bwu@ee.ryerson.ca).

Digital Object Identifier 10.1109/JSYST.2016.2563979

I. INTRODUCTION

RECENTLY, the wind energy is receiving much attention from researchers who work on finding environmentally friendly ways to produce electricity [1]. For instance, one of the leading pioneers of renewable energy industry is Denmark in which more than 30% of the total electricity consumption is supplied through renewable energy units by the end of 2010. Interestingly enough, the energy production policies of Denmark state that they will achieve to above 50% electricity using wind farm generations by the end of 2020 [2]. Widespread use of wind farms forces the power system to restructure of which the grid can accept a large amount of wind farm injections. Predictably, the power system is faced with the challenge of frequency control problem.

There are several ways to control the system frequency incorporating considerable amount of wind farm generations, one of which is to produce the sufficient power reserve. In order to create an adequate amount of the power reserve through the system, it is necessary to utilize wind farms which are capable of changing their output power. Therefore, this paper considers the wind farm containing the doubly fed induction generator (DFIG), and permanent magnet synchronous generator (PMSG) [3]–[5].

Many investigations have suggested ways to increase the participation of wind farm in order to control the system frequency. In [6] and [7], two quite similar approaches have been proposed to cope with the frequency control issue using the DFIG-based wind power generation. In this case, the appropriate frequency response has been obtained through the inertia control, and the

primary frequency control, consecutively. For another example, Lalor *et al*. and Morren *et al*. in [8] and [9] present a new approach sampling the system frequency by which power electronic converters become sensitized to frequency variations. Then, wind farm converters inject the available amount of inertia into the system to ameliorate the frequency condition. Not long after the previous investigations, it was the first time that authors introduce a novel deloading scheme to produce the power reserve in [10]. In this method, the power reserve is made by a droop control of the wind output power. Unlike the reduction of maximum frequency variations, the deloading scheme is not competent to decrease the slope of frequency variations. Then, [11] proposed a new integrative model of the frequency control to coordinate wind farms with conventional power plants perfectly. In this structure, the wind farm participates to maintain the inertia at a desirable rate and a defined participation factor compensates the lack of wind output power using the increase of conventional unit generation. The fact remains that in this integrative structure, the wind farm generations do not take part in the control of the steady-state frequency response similar to the supplementary frequency control.

Recently, the frequency control in the case of high wind farm penetration has been attracting an overwhelming majority of attention [12]. In [13], the improvement of frequency response is achieved by an optimal proportional integral (PI) controller on the condition of 5% to 50% of wind farm power injection. Also, Li *et al*. in [14] suggest an additional damping strategy in the DFIG-based wind farm in addition to the frequency control throughout the two-area power system. As another example, [15]–[17] presents a new approach, coordinating energy storage system with the wind unit in a small size power system. Furthermore, Burlibas and Ceangă propose a new synthetic method in order to improve the system dynamics and control the frequency effectively [18]. Also, in [19] the authors introduce a modern algorithm which can handle the amount of kinetic energy existing in the wind farm in order to primary frequency control. In all above investigations, wind units are operated at their maximum output rate on which there is no participation to generate the steady-state demand, and supplementary control of the system frequency. Operating on the maximum output power value obstructs the additional inertia made by the wind farm. Then, the lack of adequate wind farm participation apparently poses the problem regarding to control the system frequency during the steady-state condition.

Despite of the previous practical frequency control strategies incorporating the wind farm generation, there is no assessment how to increase the existing inertia in the case of the high penetration of wind farms. In this case, the existing inertia of the wind farm is not sufficient to support the system inertia. It needs to increase the insufficient wind farm inertia in order to participate the wind farm in the supplementary control strategy, similar to conventional power plants. Usually, a way to achieve this aim is to operate the wind farm below its maximum power rate. In this way, the increase of turbine speed which declines the wind turbine lifetime is more likely to happen. Unfortunately, the DFIG and the PMSG are not permitted to operate in the overspeed mode [20]. Quite similar to [11], to avoid the overspeed operating mode in the proposed model, the wind turbine speed is limited to an appropriate value by the blade angle pitch control. Compared to the method presented in [11], in the proposed approach in this paper, it is permitted to determine the deloading value and, therefore, keep away the turbine speed from reaching to the overspeed mode. In order to the system frequency evaluation, this paper uses the renowned load frequency control (LFC) model. Prior to the proposed model, the LFC has integrated wind units with conventional power plants in one-area and two-area power systems [10], [13], [21]. Last but not least, the design and optimal grid-connected microgrid operation is presented in [22]. In this case, wind power generation is one of the power supplies. Also in this research, uncertainty, risk exposure, robustness, and flexibility indices are evaluated. However, in the previous investigations, there is no wind farm participation whatsoever to produce the steady-state power and excessive inertia generation. Moreover, this paper presents a new control strategy for the wind farm through the LFC model incorporating conventional power plants.

This paper presents a method to produce a desirable power reserve being available in both steady state and transient conditions. Achieving to this aim, a PID controller is defined within the proposed model. The coefficients of the PID controller influence on the amount of inertia, damping, and supplementary control of the wind farm. Because of the nonlinear behavior of the frequency response, it is necessary to find the global optimum coefficients of the PID controller and the deloading factor to obtain an enough available optimal power reserve value. In this paper, the particle swarm optimization (PSO) algorithm is employed to determine the best value of coefficients using a multiobjective cost function. To show the powerful performance of the proposed model, it is applied to a well-known two-area power system. Finally, simulating results will be compared to some previous models of the wind farm.

The main contributions of this paper are as follows:

1) a novel control method of wind farm;
2) a description of frequency control method;
3) a dynamic model of LFC with wind farm.

II. Description Control Method of Wind Farm

A. Architecture PMSG-Based Wind Turbine

The typical structure of a wind turbine based on a multipole PMSG and the controller scheme are demonstrated in Fig. 1. This configuration consists of a wind turbine, a PMSG, power converters, and a transformer for grid connection. The control of a PMSG includes generator-side active power control with maximum power point tracking (MPPT), grid-side reactive power control, and dc voltage control for voltage source converters or dc current control for current source converters. The use of full-capacity converters allows the control for the generator- and grid-side converters to be decoupled, which facilities the system design and increases the operating range of the generator [3]–[5].

The excitation of a PMSG is provided by the permanent magnets, and so, no rotor winding is needed. Compared to the generators with excitation winding on the rotor, the PMSG has the

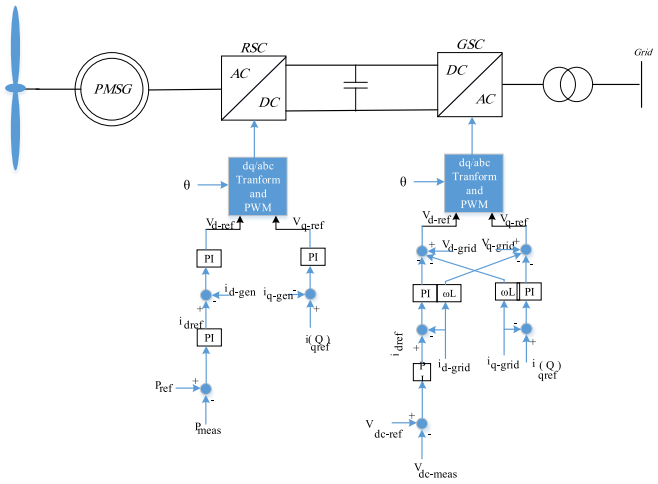

Fig. 1. Basic configuration of a permanent magnet synchronous generator.

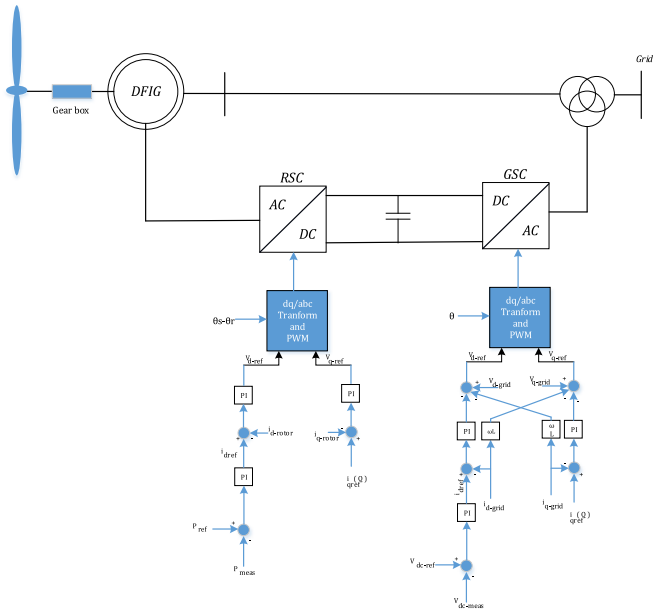

Fig. 2. Basic configuration of a doubly fed induction generator.

benefit of lower rotor losses, smaller sizes of the rotor, simpler cooling circuit, and decreased failures. However, the costs for manufacturing the permanent magnets are very high, and an appropriate cooling system is required since the permanent magnets are sensitive to high temperatures [3]–[5].

The controllable IGBTs permit the generator-side converter to handle the generation operation. Compared to the generator-side converter, the grid-side converter could control the dc-link voltage, thus exporting the active and reactive powers to the power system [3]–[5].

B. Architecture DFIG-Based Wind Turbine

The DFIG generator is commonly used in today's wind farm. The DFIG is basically a wound rotor induction generator in which the rotor circuit can be controlled by power electronic device to provide variable speed operation. A typical structure of the DFIG unit is shown in Fig. 2. The stator of the generator is connected to the grid through a transformer, while the rotor connection to the grid is done through back-to-back converter and the transformer [3]–[5].

The stator of the DFIG generator provides power from the wind turbine to the grid and, therefore, the power flow is unidirectional. However, the power flow in the rotor circuit is bidirectional, depending on the operating situations [1]. The power can be provided from the rotor to the grid and contrariwise through rotor side converter (RSCs) and grid side converters (GSCs). Since the maximum rotor power is almost 30% of the rated stator power, the power rating of the converters is significantly decreased in comparison to the PMSG with full-capacity converters [3]–[5].

The back-to-back converter permits the operator to control the electromechanical torque and the rotor excitation. The size of the converter depends on the generator rating, usually in the range between 15% and 30%. As the power converter operates in a bidirectional way, the DFIG can be operated either in subsynchronous or in supersynchronous operational mode.

C. Control of Converter

RSC: RSCs change the rotor's ac voltage into dc voltage by active and reactive power control. The active power which is determined by frequency regulation control and the reactive power which is controlled and assigned by the power system operator are compared with the measured ones of the terminal of the unit [3]–[5].

GSC: GSCs change the dc bus voltage to ac voltage using pulse width modulation through voltage oriented control with a decoupled controller. It controls the reactive power output and also the dc bus voltage of the wind unit. DC bus voltage and reactive power output are defined by the power system operator [3], [5].

III. Description of Frequency Control Method

Wind blade power from wind speed is described by the following:

$$P_{\text{opt}} = \frac{1}{2}\rho C_P(\lambda,\beta)AV_\omega^3. \tag{1}$$

Then, CP could be expressed as a function of the tip speed ratio λ and the blade pitch angle β given by (2) [23]

$$C_P(\lambda,\beta) = (0.44 - 0.0167\beta)\sin\frac{\pi(\lambda-2)}{13-0.3\beta} - 0.00184 \times (\lambda-2)\beta \tag{2}$$

$$\lambda = \frac{\omega R}{V\omega}. \tag{3}$$

To achieve a permanent wind farm participation in order to control the system frequency, it is mandatory to produce a power reserve with quick reaction during a long period of time. Generating such power reserve, it needs to operate the wind farm in a deloading state. The deloading state operation violates the permissible speed range, namely the wind turbine speed reaches to overspeed region. To avoid the overspeed problem, the wind turbine speed is handled by the blade angle pitch control scheme.

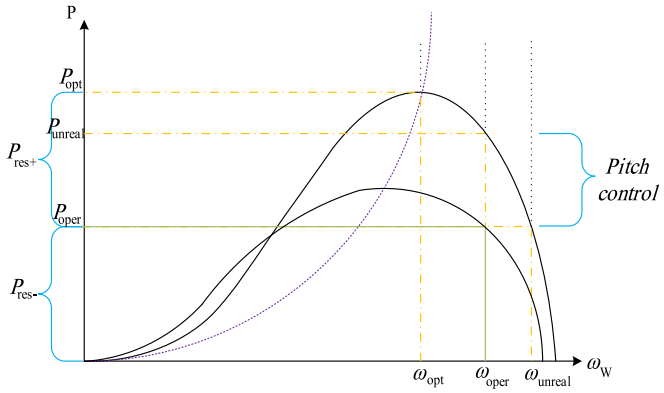

Fig. 3. Wind turbine power-speed characteristic.

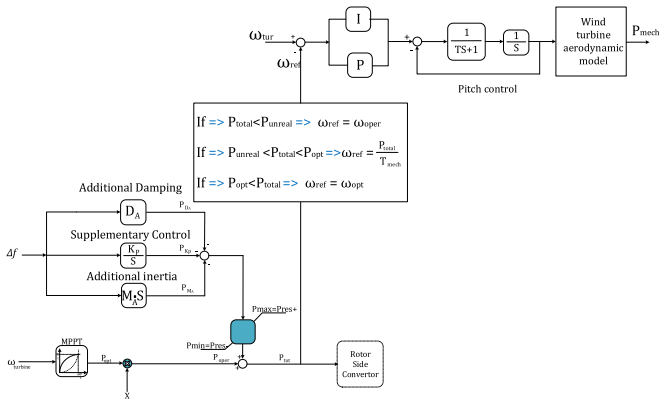

Fig. 4. Proposed control scheme of RSCs.

According to the wind turbine power-speed characteristic shown in Fig. 3, if the wind farm is operated at the $\mathrm{P_{oper}}$ point, the $\mathrm{P_{res}}^{+}$ value is stored within the wind farm. Deliberately, the blade angle pitch control scheme provides for the wind farm to be operated at the ω_{oper} speed value instead of the ω_{unreal} turbine speed. Consistent with this idea, the positive reserve and the negative reserve of the wind farm can be specified by a distinct factor X as follows:

$$0 \leq X \leq 1 \tag{4}$$

$$P_{\mathrm{res}+} = P_{\mathrm{opt}}(1-X) \tag{5}$$

$$P_{\mathrm{res}+} = XP_{\mathrm{opt}}. \tag{6}$$

In order to have fast response from the power reserve, a method is proposed to control the wind units. The proposed method shown in Fig. 4 shows the modulation of the RSCs.

In the lower branch, MPPT determines the maximum power through a sampling of the wind speed, and then by using coefficient X the value of operation power is specified.

Within the middle branch, a PID controller is designed to control the wind farm frequency. The PID coefficients are: 1) M_A determines the wind farm inertia, 2) D_A specifies the amount of wind farm damping, and 3) K_{P} symbolizes the supplementary control which decides the steady-state output variation of the wind farm.

As previously pointed out, the speed of wind turbine and generator can increase within a permissible range. At this speed range, the lifetime of mechanical equipment, embedded in wind farm units, subsides providing that the speed of turbine increases. Then, the upper branch, according to Fig. 4, retains control of turbine speed continuously at the ω_{oper} rate. Also, the turbine speed is regulated at the ω_{opt} speed rate as long as the $\mathrm{P_{total}}$ output power value becomes less than the optimal power of wind unit. Fig. 4 indicates when the wind unit output amounts to a value within ($\mathrm{P_{unreal}}$,$\mathrm{P_{opt}}$), the turbine speed can be determined according to the power and torque equation illustrated in Fig. 4.

Therefore, there is no limitation to produce the reserve power for a typical wind farm through the proposed control scheme. For example, the wind power can be operated at the half of its maximum rate so long as the X parameter is 0.5 value. In this case, the blade angle pitch control scheme inhibits the turbine speed from growing as much as it is allowed.

The control circuit has three branches, that the wind unit output power is determined as follows:

$$P_{\mathrm{total}} = P_{\mathrm{oper}} + P_{M_A} + P_{D_A} + P_{K_P}. \tag{7}$$

IV. Dynamic Model of LFC With Wind Farm

The conventional unit's frequency control model includes inertia control, droop control, and supplementary control. This model is shown in the upper part of Fig. 5. In the conventional units, the rotating masses (generator and turbines) inertia prevents the rapid changes of frequency. Therefore, sufficient time is provided to compensate the added load power by the generators using governor and supplementary control [24].

The proposed dynamic model of LFC with wind farm is illustrated in Fig. 5. The wind units and the conventional power plants are depicted in the upper part and lower part of the diagram, respectively. Throughout the frequency control of wind farm, the integral controller, washout filter, and the PID controller can determine the active power variation value in different situations.

A reference power which forces the speed to track a desired reference speed is computed as follows [11]:

$$P_m = k_P(\omega^*_{ref} - \omega_m) + k_I \int (\omega^*_{ref} - \omega_m)dt. \tag{8}$$

The power difference between the mechanical power (P_{m}) and electrical power (P_{e}) creates the rotor acceleration relationship as follows [24]:

$$P_m - P_e = J\omega_m \frac{d\omega_m}{dt}. \tag{9}$$

According to Fig. 5, the power changes for frequency control are obtained as follows:

$$\Delta P_{\mathrm{FC}} = P_{M_A} + P_{D_A} + P_{K_P}. \tag{10}$$

The wind power variation can be formulated as follows:

$$\Delta P_{\mathrm{wind}} = \Delta\beta\frac{dp}{d\beta} + \Delta\omega\frac{dp}{d\omega} + \Delta V\frac{dp}{dV} \tag{11}$$

where $\mathrm{dp/d}\beta$ is the wind output variation for a specific change of blade angle, $\mathrm{dp/d}\omega$ is the proportion of wind power variation

to the small change of turbine angular speed, and dp/dV means the wind output variation for a definite wind speed variation. All these implicit derivative terms can be obtained by the following formulations:

$$\frac{dp}{d\beta} = \frac{1}{2}\rho A V_\omega^3 \frac{dc_p}{d\beta} \tag{12}$$

$$\frac{dc_p}{d\beta} = 0.167 \sin\frac{\pi(\lambda-2)}{0.3\beta-13} - \left[\frac{0.3\pi(\lambda-2)}{(0.3\beta-13)^2} \times \cos \times \left(\frac{\pi(\lambda-2)}{(0.3\beta-13)}\right) \times (0.167\beta - 0.44)\right] - 0.00184(\lambda-2) \tag{13}$$

$$\frac{dp}{d\omega} = \frac{1}{2}\rho A V_\omega^3 \frac{dc_p}{d\lambda}\frac{d\lambda}{d\omega} \tag{14}$$

$$\frac{dc_p}{d\lambda}\frac{d\lambda}{d\omega} = \left[\frac{R}{V_\omega}\right] \frac{\pi}{(0.3\beta-13)} \times \cos\left(\frac{\pi(\lambda-2)}{(0.3\beta-13)}\right) \times (0.167\beta - 0.44) - 0.00184\beta \tag{15}$$

$$\frac{dp}{dV} = \frac{3}{2}\rho A C_P V_\omega^2. \tag{16}$$

The act of sampling from the network frequency variations is done by means of an element being dilatory. As this time delay influences on the frequency controller function, it is important to consider the mentioned delay in the modeling stage. Subsequent to the frequency sampling step, the washout filter is employed in order to prevent the low-frequency oscillation entrance. Finally, the PID controller makes the wind farm aware of power variations.

Then, this power variation is injected into the system immediately by means of available wind farm inertia, including the mechanical inertia loop and the speed regulator. Mauricio *et al*. in [11], [13], and [18] gives more details about the modeling of inertia loop control and the wind speed regulator. Then, the variation of turbine speed $(\Delta\omega)$ specifies the blade angle variation value $(\Delta\beta)$ using the pitch angle control loop. Afterward, the wind power variations determine the available amount of input power, according to (11). It is worth to say that the wind output power variations depend on the turbine speed variations $(\Delta\omega)$, the value of blade angle $(\Delta\beta)$, and the wind speed changes. Next, the (9) subtracts the output power from the available input power, thereby obtaining the turbine speed variations $(\Delta\omega)$. Using the turbine speed variations $(\Delta\omega)$, the output power variation value can be calculated from (8) of which the PI controller applies this variation to the current output power.

Additional inertia, additional damping, and spinning reserves have been modeled in the frequency control part of Fig. 5. By deriving the changes of system frequency, the additional inertia is created for wind units using $M_{A.}$ In addition, K_P determines the steady-state power change for the wind units. This coefficient specifies the permanent wind farm partnership in the frequency control. Additional damping is produced using the frequency change Δf and D_A. Finally ΔP_{FC} is determined by applying to the rotor-side convertor and a limiter.

V. Mathematical Formulation and the Implementation of PSO

Now for the effective performance of the proposed frequency control strategy, it is necessary to determine the best value of the frequency control gains (M_A,D_A, and K_P) in addition to the deloading of the wind farm (X). In the other hand, the optimal adjustment of frequency control parameters provides a desirable frequency response in the case of the fewest deloading factor values.

There are four influential parameters which can improve frequency response features. As previously mentioned, the availability of power reserve is a prerequisite for the wind farm to have a collaborating role in the system frequency control plan. Boasting the sufficient power reserve, the wind farms need to generate the active power lower than their maximum output power. However, the decrease of wind farm output power is not compatible with the economic aspect of wind farm operation. Practically, it is economical to operate the wind farm close to its maximum output power. Consequently, it is essential to optimize the deloading factor value according to the economic aspect, and required power reserve. Second, the M_A parameter decides the increase of the wind farm inertia level. Generally, a high amount of M_A parameter could help to achieve a frequency response with smooth variations. Third, the increase of D_A parameter can modify the damping of the frequency response. Further, the K_P parameter in the proposed model plays a role as a supplementary control parameter of the wind farm. This parameter has an effect on settling time (ST) of the frequency response, directly.

It is worth to say that is not appropriate to adjust the above parameters alone. Indeed, M_A,D_A, and K_P parameters are the coefficients of a PID controller throughout the proposed model. Probably, the value of coefficients in a PID controller adds a certain pole and zero to the transfer function of the model. Then, the frequency response manner is dependent on the relative location of the added pole and zero. As a consequence, it is crucial to determine the optimal amount of parameters simultaneously in order to reach a desirable frequency response. In the other hand, the problem is to find an optimal combination of the unknown parameters to optimize some certain system characteristics. In this study, a multiobjective function is considered to find the best value of parameters for the proposed frequency control scheme as follows:

$$\mathrm{OF}(K_P, D_A, M_A) = \alpha \times X + \beta \times \int |\Delta f|^2 dt + \gamma \times \mathrm{ST} + \sigma \times \mathrm{MSFC} \tag{17}$$

where X is the deloading factor of the wind farm, $\int^{\Delta} f^2 dt$ is the integral squared error of the frequency, ST is the settling time of the response, and MSCF is the maximum slope of the frequency response. The permissible ranges of the above parameters are

$$0 \le X \le 0.15 \tag{18}$$

$$50 \le M_A \le 90 \tag{19}$$

$$50 \le D_A \le 90 \tag{20}$$

$$0 \le K_P \le 10. \tag{21}$$

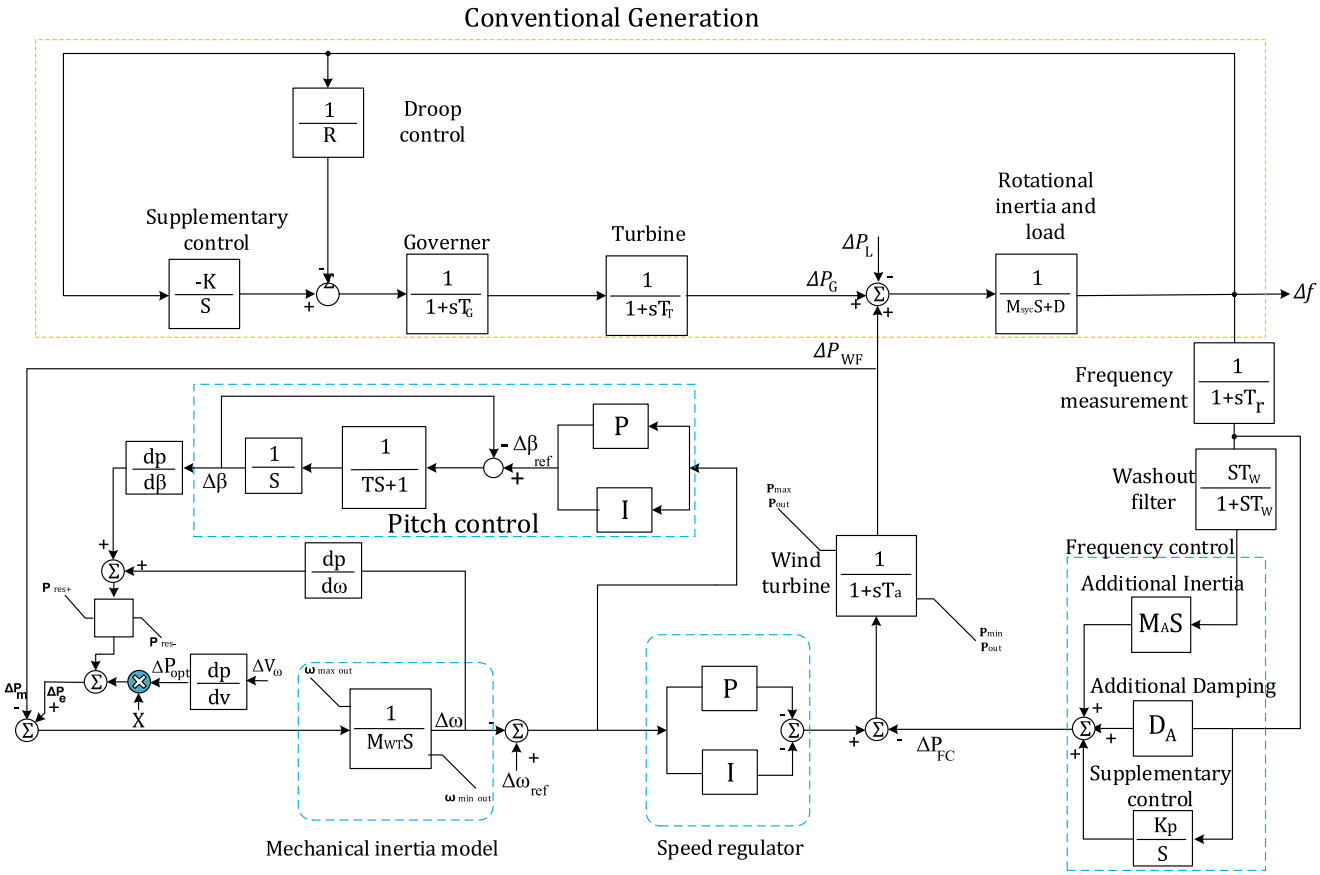

Fig. 5. Dynamic model of an LFC with wind farm.

In the PSO algorithm, there are two main parameters which define the size of search space. One is the number of populations and another is the number of individuals in each population. In the PSO algorithm, the number of population is arbitrary that can be chosen based on the designer's vision. However, the number of individuals in each population is certain and equals to the number of unknown parameters that is 3 in this problem. So, if the number of populations specifies by n and the number of unknown parameters equals to m, the search space is a matrix with the dimensions of n × m in which each element represents a coefficient of PID controller. So, the search space matrix can be represented as

$$X_{\text{Search}-\text{space}} = [x_{ij}]_{\text{n}\times\text{m}}. \tag{22}$$

Throughout the initial process of PSO algorithm, a generating process of random number sets a value for each element of search space while all inequality constraints, namely (18)–(21), are satisfied. After that it is time to move the particles to the best position in which the multiobjective function introduced in (17) is at its minimum point. The velocity vector of PSO algorithm is defined as follows:

$$\begin{aligned} V_k^{k+1} = \; & wV_i^k + c_1.\,rand_1\,.\,(Pbest_i^k - X_i^k) \\ & + c_2.\,rand_2\,.\,(Gbest_i^k - X_i^k) \end{aligned} \tag{23}$$

where V_i^k is velocity of individual i at iteration k, w is the weight parameter, c_1 and c_2 are weighted factors, rand_1 and rand_2 are random numbers between 0 and 1, X_i^k is the position of individual i, $Pbest_i^k$ is the best position of individual i until iteration k, and $Gbest_i^k$ is the best position of the group until iteration k. The individual moves from the current position to the next position by

$$X^{k+1} = X^k + V^{k+1}. \tag{24}$$

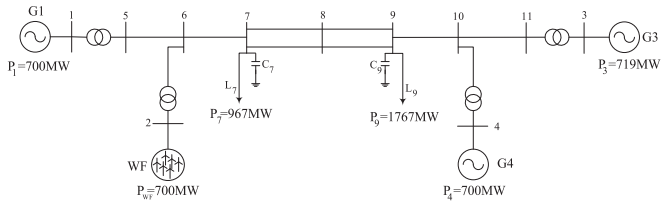

Fig. 6. Two-area three-generator test system with wind farm at bus.

VI. Simulation Results

As shown in Fig. 6, the power system used for this simulation is taken from [23, Example 12.6]. As seen, the power system has two areas. The area-1 consists of one 900-MVA conventional generator, one 900-MVA wind farm with specification as noted in Table I, and a load of 967-MW which is connected to the bus 7. The second area consists of two 900-MVA conventional generators and a load of 1767-MW that is connected to the

TABLE I
MODEL CONSTANTS USED FOR CASE STUDY

Symbol	Description	Value
M_{wu}	Equivalent wind unit inertia	4.5 s
T_A	Wind turbine time constant	0.2 s
k_p	Speed regulator proportional constant	5
k_i	Speed regulator integral constant	100
k_p	Pitch angle control proportional constant	50
k_i	Pitch angle control integral constant	150
M_A	Additional inertia	73.51
D_A	Additional damping	58.8
K_P	Supplementary gain	9.85
X	de-loading factor	0.105

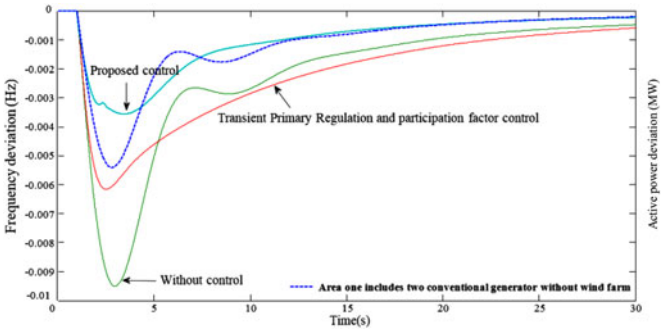

Fig. 7. Frequency variation for different control methods.

bus 9. Also, these two areas are connected together by a tie line between buses 7 and 9.

In this case study, the load connected to bus 7 increases in the amount of 180 MW at a time instant of 1 s. This increment causes a sharp drop in frequency due to the 50% penetration of the wind farm. Simulations have been performed in four cases, including

1) The wind farm has been replaced by a 900-MVA conventional generator in the first area.
2) The power system illustrated in Fig. 6 is simulated and there is no frequency control implementation.
3) The system shown in Fig. 6 is simulated with the primary frequency regulation and participation factor control (PFRPFC).
4) The proposed strategy is applied to the case study.

Fig. 7 shows the frequency changes throughout the area-1 of the case study regarding the four predefined states. First, the power system shown in Fig. 7 is evaluated without the wind farm penetration of which its frequency response is shown by the dotted line curve. As it is shown, the frequency response has a maximum variation of –0.0055. In the second stage, the case study is assessed incorporating 50% of the wind farm penetration. The simulation results indicate that the replacement of a wind farm with a conventional power plant reduces the slope of frequency collapse and the minimum value of the frequency. The frequency response undergoes a maximum variation of –0.0094 when the wind farm is replaced. In comparison with the conventional power plant, the frequency drop has become twice. Using the method introduced in [11], the available wind

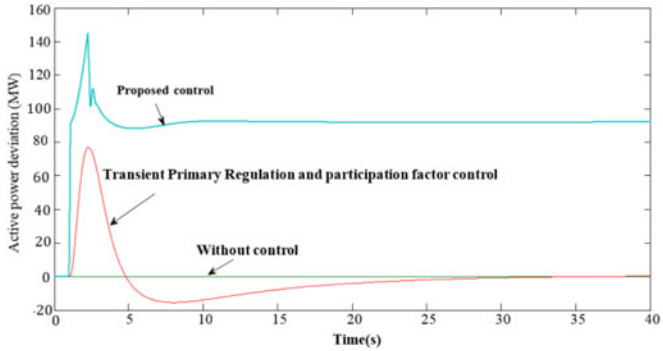

Fig. 8. Active power deviation injected by wind farm for different control methods.

farm inertia is injected into the network by which the minimum frequency value and the frequency curve slope are improved approximately. Equally importantly, this control scheme improves the frequency changes to –0.00612 while it is more than that of conventional power plant. Another point is that the maximum frequency value has been occurring at 2.9 s throughout the three previous simulations.

However, the slope of frequency response is very high. Therefore, the method presented in [11] lacks capability to replace a wind farm with a conventional unit. Finally, the wind farm is simulated with the proposed control strategy. Comparing the results, one can find out that the frequency response experiences an amelioration concerning the amount of frequency slope, the minimum frequency value, and the ST. These advantages attributes to the power injection of the wind farm through which the network inertia and the system damping value are increased. Using the proposed strategy, the maximum frequency deviation comes to –0.00355. This value is less than the value of frequency response shown in dotted line. Also, the maximum value point has been happened in 3.5 s which this increase of time proves the increase of system inertia. Further, the results show a powerful participation of the wind farm in the frequency supplementary control. It is concluded that the proposed scheme is a viable solution to replace a wind unit with an existing conventional power plant without the frequency perturbation.

From the wind farm output power point of view, the output variation is zero in the case of no control strategy. Fig. 8 illustrates that there is not any wind farm participation in the frequency control. In order to compare the proposed strategy to the PFRPFC presented in [11], this method is applied to the case study. The PFRPFC changes the wind farm output for a specific load variation value. Unfortunately, this method makes a power change with a low pace. This slow variation provides a steep slope collapse of frequency. Furthermore, through the PFRPFC, the power variation continues in a short period of time and the wind farm cannot vary its output power throughout the steady state. The maximum power injection through this approach equals to 79 MW while this power injection reaches to zero value after the oscillation in 40 s.

Through the proposed method, the power variation steepens sharply; as a result, it makes the frequency drop slope smooth. As shown in Fig. 8, the power increase continues with a sharp

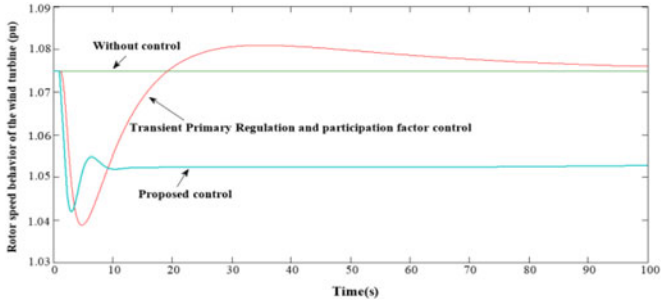

Fig. 9. Wind turbine rotor rotation speed for different control methods.

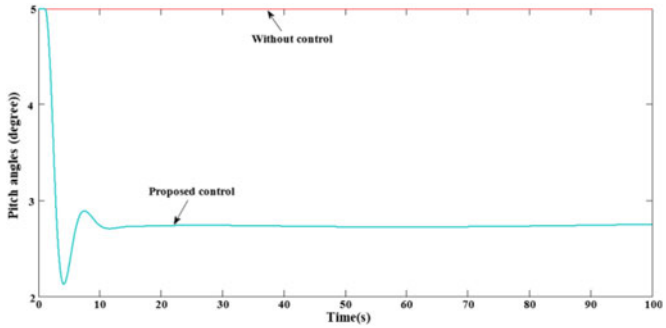

Fig. 10. Pitch angles behaviors of the wind turbine for different control methods.

slope until 90 MW. This high slope exists because of the available active power within the wind farm inertia. When the power increases above 90 MW value, the slope becomes smooth rather than that of the previous phase, that is the amount of active power was below 90 MW. This surplus active power, the amount of active power more than 90 MW, is generated by the generator speed reduction and cutting the angle of blades. So, it is not possible to inject the wind farm inertia into the system swiftly. After a 10-s time interval, as shown in Fig. 8, the power variation during the steady state is provided by the generator speed and the blades angle reduction. The wind farm supplies around 90 MW active power in the steady state that is 50% participation of the wind farm.

Regarding the rotor speed variation, the results are shown in Fig. 9 for various control approaches. On the condition of no control scheme, there is not any power change relating to the wind farm output. Therefore, the speed of wind turbines has a constant value. Through the PFRPFC when the active power increases, the speed of wind turbines decreases. Consistent to this idea, the speed of wind turbines comes to zero value. In comparison with the PFRPFC, the proposed method offers a condition by which the slope of frequency drop is steeper than that of the PFRPFC. This obtained steep slope is made by the high slope power injection. In addition, the speed reduction makes it possible to achieve a considerable participation of the wind farm in the steady-state active power control.

Despite the lack of controller for the blade angle pitch control in the PFCPFR, the proposed strategy employs a controller in order to readjust the angle value of blades when it is needed. This PI controller regulates blade angle values if the speed of turbine changes. Fig. 10 shows the β angle variations of which the angle value reduces as long as the load demand increases. Then, the amount of blade angle remains constant during the steady state in order to increase the active power value. As shown in Fig. 10, the maximum blade angle variation is –2.3 degree which approaches to –2.3 degree in the case of steady state.

As stated earlier, there is a clear consensus on the nonlinear behavior of frequency response when there are different PID coefficients. Another way to say this is that the improvement of frequency response is dependent upon the value of PID parameters. Conceivably, the inappropriate adjustment of PID parameters has some adverse bearings on the frequency response. Avoiding this problem, the need to design an optimal PID controller arises. In this part by employing the PSO algorithm and

TABLE II
SIMULATION RESULT OBTAINED BY THE PSO ALGORITHM IN THE FIRST CASE, ITERATION $= 20$, POPULATION $= 50$, NUMBER OF PROGRAM RUNNING $= 10$

	OF	X	M_A	D_A	K_P
Best	0.0326	0.1084	88.5470	56.6636	10.0000
Average	0.0332	0.1053	67.8173	53.4232	9.7294
Worst	0.0340	0.0995	59.3743	53.4232	9.2248

TABLE III
SIMULATION RESULTS RELATED TO THE SECOND SCENARIO OF THE OPTIMIZATION, ITERATION $= 50$, POPULATION $= 100$, NUMBER OF PROGRAM RUNNING $= 10$

	OF	X	M_A	D_A	K_P
Best	0.0320	0.1106	85.4386	51.3101	9.8662
Average	0.0328	0.1089	72.7014	53.5194	9.9313
Worst	0.0332	0.1082	72.7786	53.1988	9.9102

the predefined objective function in (17), the optimal adjustment of PID coefficients is analyzed through two following cases: in the first case the population and iteration of PSO method are 20 and 50, respectively. In another case, the population and iteration are adjusted to 50 and 100 in order to evaluate the effect of search space on the proposed PID controller performance. Table II shows the simulation results regarding the first optimization case, when the optimization process is applied to the system ten times. The best, the worst, and the average values of the multiobjective function approve of the power performance of PSO algorithm in several aspects. One is that as the best value and the average value of the objective function do not differ widely from each other, this means that there is few scattering among the obtained results through different program running. It is a major characteristic for each optimization scheme to acquire the minimum scattering among a multitude of program running. As shown in Table II, the objective function best value is 0.0326 compared to the average value of 0.0332 which is near to the best value.

According to the second case results, shown in Table III, there is a suitable performance of the proposed optimization process again. Furthermore, the second case indicates that the search space of PSO algorithm is a meant to broaden the PID controller

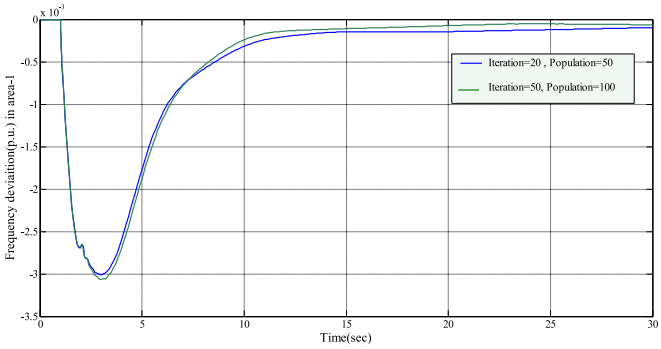

Fig. 11. Best frequency responses using the best values of PID coefficients obtained by the PSO algorithm in two different cases.

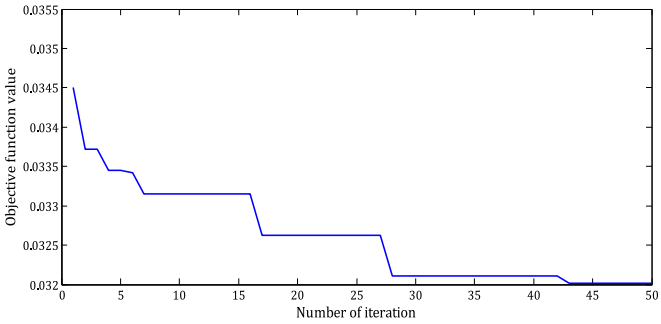

Fig. 12. Convergence curve of the PSO method while the number of iteration= 50, and the number of generation= 100.

TABLE IV
SIMULATION RESULTS OBTAINED BY DE ALGORITHM, ITERATION = 50, POPULATION = 100, NUMBER OF PROGRAM RUNNING = 10

	OF	X	M_A	D_A	K_P
Best	0.0331	0.1006	57.4016	54.7788	8.6661
Average	0.0346	0.1054	61.4033	56.0017	9.004
Worst	0.0350	0.1083	72.7786	58.3221	9.5

efficiency. In this case, the best value of the objective function is fewer than that of the first case. Fig. 11 compares the optimal frequency response obtained by the two predefined cases in their best values. In order to justify that the obtained parameters are optimal, the convergence curve of the PSO method is shown in Fig. 12. To assess the performance of PSO algorithm, the optimal parameters are calculated using the differential evolutionary (DE) algorithm, shown in Table IV. In this case, the number of iteration and the population are 50 and 100, respectively. Similar to the previous stage, the program is performed for ten times. By comparing the results, shown in Tables III and IV, one can find out that the PSO algorithm could succeed in finding the optimum point of the objective function. As it is stated, the best result of PSO algorithm is 0.0320, in comparison with the best result of DE algorithm that is 0.0331. Interestingly enough, the scattering of results in the PSO algorithm is less than that of the DE algorithm. As it is seen, the difference between the best result and the average result in the PSO algorithm is 0.008.

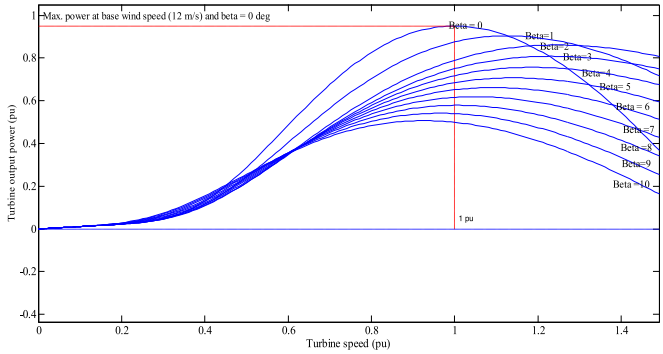

Fig. A1. Turbine power characteristic for the proposed method.

Compared to the PSO results, the difference value for the DE algorithm is 0.015. This less difference value demonstrates why the PSO algorithm is suitable for the optimization process.

VII. CONCLUSION

This paper presents a novel control scheme which helps to intensify the inertia and the damping of network incorporating high penetration of wind farms. In addition, through the proposed controlling scheme, it is possible for wind farms to participate in the supplementary frequency control. Afterward, a new LFC model of wind farms, including the proposed control strategy is presented. Then, a multiobjective function consisting of frequency response characteristics is formulated. It is aimed to find the best value of the PID coefficients by employing the PSO algorithm. Finally, the proposed method is applied to a two-area power system and the simulation results are compared to the previous control approaches. Drawing a comparison between the proposed method and the previous schemes, one can find out the viable performance of the proposed strategy.

APPENDIX

The turbine speed variation according to the power deviation in different blade angle values is shown in Fig. A1.

REFERENCES

[1] T. Malakar, S. K. Goswami, and A. K. Sinha, "Impact of load management on the energy management strategy of a wind-short hydro hybrid system in frequency based pricing," *Energy Convers. Manage.*, vol. 79, pp. 200–212, 2014.
[2] "Energy policy report 2012," Ministry of Climate, Energy and Building, Denmark, May 2012.
[3] B. Wu, Y. Lang, N. Zargari, and S. Kouro, *Power Conversion and Control of Wind Energy Systems*. New York, NY, USA: Wiley-IEEE Press, 2011, pp. 1–23.
[4] N. Ekanayake and J. Jenkins, "Comparison of the response of doubly fed and fixed-speed induction generator wind turbines to changes in network frequency," *IEEE Trans. Energy Convers.*, vol. 19, no. 4, pp. 800–802, Dec. 2004.
[5] M. Eremia and M. Shahidehpour, "Wind power generation," in *Handbook of Electrical Power System Dynamics: Modeling, Stability, and Control*. New York, NY, USA: Wiley-IEEE Press, 2013, pp. 179–228.
[6] F. W. Koch, I. Erlich, and F. Shewarega, "Dynamic simulation of large wind farms integrated in a multimachine network," in *Proc. IEEE Power Eng. Soc. General Meet.*, vol. 4, 2003, pp. 2164–2169.

[7] R. G. de Almeida and J. A. Peças Lopes, "Participation of doubly fed induction wind generators in system frequency regulation," *IEEE Trans. Power Syst.*, vol. 22, no. 3, pp. 944–950, Aug. 2007.
[8] G. Lalor, A. Mullane, and M. J. O'Malley, "Frequency control and wind turbine technologies," *IEEE Trans. Power Syst.*, vol. 20, no. 4, pp. 1905–1913, Nov. 2005.
[9] J. Morren, S. W. H. de Haan, W. L. Kling, and J. A. Ferreira, "Wind turbines emulating inertia and supporting primary frequency control," *IEEE Trans. Power Syst.*, vol. 21, no. 1, pp. 433–434, Feb. 2006.
[10] R. G. de Almeida and J. A. Peças Lopes, "Participation of doubly fed induction wind generators in system frequency regulation," *IEEE Trans. Power Syst.*, vol. 22, no. 3, pp. 944–950, Aug. 2007.
[11] J. M. Mauricio, A. Marano, A. G. Exposito, and J. L. M. Ramos, "Frequency regulation contribution through variable-speed wind energy conversion systems," *IEEE Trans. Power Syst.,* vol. 24, no. 1, pp. 173–180, Feb. 2009.
[12] D. Gautam, L. Goel, R. Ayyanar, V. Vittal, and T. Harbour, "Control strategy to mitigate the impact of reduced inertia due to doubly fed induction generators on large power systems," *IEEE Trans. Power Syst.*, vol. 26, no. 1, pp. 214–224, Feb. 2011.
[13] M. Jalali and K. Bhattacharya, "Frequency regulation and AGC in isolated systems with DFIG-based wind turbines," in *Proc. IEEE Conf. Power Energy Soc. General Meet.*, Vancouver, BC, Canada, 2013, pp. 1–5.
[14] H. Li, S. Liu, H. Ji, D. Yang, C. Yang, and H. Chen, "Damping control strategies of inter-area low-frequency oscillation for DFIG-based wind farms integrated into a power system," *Int. J. Elect. Power*, vol. 61, pp. 279–287, 2014.
[15] A. M. Howlader, Y. Izumi, A. Uehara, N. Urasaki, T. Senjyu, and A. Y. Saber, "A robust controller based frequency control approach using the wind-battery coordination strategy in a small power system," *Int. J. Elect. Power*, vol. 58, pp. 190–198, 2014.
[16] J. Pahasa and I. Ngamroo, "Coordinated control of wind turbine blade pitch angle and PHEVs using MPCs for load frequency control of microgrid," *IEEE Syst. J.*, vol. 10, no. 1, pp. 97–105, Mar. 2016.
[17] Y. Mishra, S. Mishra, and F. Li, "Coordinated tuning of DFIG-based wind turbines and batteries using bacteria foraging technique for maintaining constant grid power output," *IEEE Syst. J.*, vol. 6, no. 1, pp. 16–26, Mar. 2012.
[18] A. A. Burlibas and E. Ceangă, "Frequency domain design of gain scheduling control for large wind systems in full-load region," *Energy Convers. Manage.*, vol. 86, pp. 204–215, 2014.
[19] A. B. T. Attya and T. Hartkopf, "Control and quantification of kinetic energy released by wind farms during power system frequency drops," *IET Renewable Power Gener.*, vol. 7, pp. 210–224, 2013.
[20] V. Yaramasu, B. Wu, S. Alepuz, and S. Kouro, "Predictive control for low-voltage ride-through enhancement of three-level-boost and NPC-converter-based PMSG wind turbine," *IEEE Trans. Ind. Electron.*, vol. 61, no. 12, pp. 6832–6843, Dec. 2014.
[21] Y. Tang, Y. Bai, C. Huang, and B. Du, "Linear active disturbance rejection-based load frequency control concerning high penetration of wind energy," *Energy Convers. Manage.*, vol. 95, pp. 259–271, 2015.
[22] S. P. Ahamdi, S. N. Lordejani, A. Rahimi-Kian, A. Mohammadi Milasi, and P. M. Vahdati, "Uncertainty based configuration design and optimal operation of a grid-connected micro-grid," in *Proc. Smart Grid Conf.*, Tehran, Iran, 2013, pp. 102–107.
[23] E. N. Hinrichsen, "Controls for variable pitch wind turbine generators," *IEEE Trans. Power App. Syst.*, vol. PAS-103, no. 4, pp. 886–892, Apr. 1984.
[24] P. Kundur, *Power System Stability and Control*. New York, NY, USA: McGraw-Hill, 1993.

Vahid Gholamrezaie, photograph and biography not available at the time of publication.

Mehdi Ghazavi Dozein, photograph and biography not available at the time of publication.

Hassan Monsef (M'15), photograph and biography not available at the time of publication.

Bin Wu (S'89–M'91–SM'99–F'08), photograph and biography not available at the time of publication.